

Improved signal-to-noise ratio of 10 GHz microwave signals generated with a mode-filtered femtosecond laser frequency comb

S. A. Diddams¹, M. Kirchner¹, T. Fortier¹, D. Braje¹,
A. M. Weiner², and L. Hollberg^{1,3}

¹*Time and Frequency Division, National Institute of Standards and Technology,
Boulder, CO 80305*

²*Department of Electrical and Computer Engineering, Purdue University,
West Lafayette, IN 47907-1285*

³*Current address: 5052 N. Foothills Hwy., Boulder, CO 80302*

sdiddams@boulder.nist.gov

Abstract: We use a Fabry-Perot cavity to optically filter the output of a Ti:sapphire frequency comb to integer multiples of the original 1 GHz mode spacing. This effectively increases the pulse repetition rate, which is useful for several applications. In the case of low-noise microwave signal generation, such filtering leads to improved linearity of the high-speed photodiodes that detect the mode-locked laser pulse train. The result is significantly improved signal-to-noise ratio at the 10 GHz harmonic with the potential for a shot-noise limited single sideband phase noise floor near -168 dBc/Hz.

© 2009 Optical Society of America

OCIS codes: (350.4010) Microwaves; (250.0040) Detectors; (320.7160) Ultrafast technology.

References and links

1. A. Bartels, S. A. Diddams, C. W. Oates, G. Wilpers, J. C. Bergquist, W. H. Oskay, and L. Hollberg, "Femtosecond-laser-based synthesis of ultrastable microwave signals from optical frequency references," *Opt. Lett.* **30**, 667–669 (2005).
2. J. J. McFerran, E. N. Ivanov, A. Bartels, G. Wilpers, C.W. Oates, S. A. Diddams, and L. Hollberg, "Low-noise synthesis of microwave signals from an optical source," *Electron. Lett.* **41**, 36–37 (2006).
3. M. I. Skolnik, *Radar Handbook, 3rd Edition*, McGraw-Hill (New York, 2008).
4. G. Santarelli, Ph. Laurent, P. Lemonde, A. Clairon, A. G. Mann, S. Chang, A. N. Luiten, and C. Salomon, "Quantum Projection Noise in an Atomic Fountain: A High Stability Cesium Frequency Standard," *Phys. Rev. Lett.*, **82**, 4619–4622 (1999).
5. A recent review of the work in this field is found in: *Special issue on microwave photonics*, *J. Lightwave Tech.*, **26** 2336–2810 (2008).
6. E. N. Ivanov, S. A. Diddams, and L. Hollberg, "Analysis of noise mechanisms limiting the frequency stability of microwave signals generated with a femtosecond laser," *IEEE J. Sel. Top. Quantum Electron.* **9**, 1059–1065 (2003).
7. E. N. Ivanov, S. A. Diddams, and L. Hollberg, "Study of the excess noise associated with demodulation of ultra-short infrared pulses," *IEEE Trans. Ultrasonics, Ferroelectrics and Freq. Control* **52**, 1068–1074 (2005).
8. T. Ozeki and E. H. Hara, "Measurement of nonlinear distortion in photodiodes," *Electron. Lett.* **12**, 81–82 (1976)
9. K. J. Williams, and R. D. Esman, "Observation of photodetector nonlinearities," *Electron. Lett.* **28**, 731–732 (1992).
10. K. J. Williams, R. D. Esman, and M. Dagenais, "Effects of high space-charge fields on the response of microwave photodiodes," *IEEE Photon. Technol. Lett.* **6**, 639–641 (1994).
11. D. A. Tulchinsky and K. J. Williams, "Excess amplitude and excess phase noise of RF photodiodes operated in compression," *IEEE Photon. Technol. Lett.* **17**, 654–656 (2005).

12. M. Currie and I. Vurgaftman, "Microwave phase retardation in saturated InGaAs photodetectors," *IEEE Photon. Technol. Lett.* **18**, 1433-1435 (2006).
13. Y. Liu, S.-G. Park, and A. M. Weiner, "Enhancement of narrow-band terahertz radiation from photoconducting antennas by optical pulse shaping," *Opt. Lett.*, **21**, 1762-1764 (1996).
14. S.-G. Park, A. M. Weiner, M. R. Melloch, C. W. Siders, J. L. W. Siders, and A. J. Taylor, "High Power Narrow-Band Terahertz Generation Using Large Aperture Photoconductors," *IEEE J. Quantum Electron.*, **35**, 1257-1268 (1999).
15. J. Chou, Y. Han, and B. Jalali, "Adaptive RF-photonics arbitrary waveform generator," *IEEE Photon. Technol. Lett.* **15**, 581-583 (2003).
16. I. S. Lin, J. D. McKinney and A. M. Weiner, "Photonic synthesis of broadband microwave arbitrary waveforms applicable for ultra-wideband communication," *IEEE Microwave Wirel. Compon. Lett.* **15**, 226-228 (2005).
17. J. D. McKinney and A. M. Weiner, "Compensation of the effects of antenna dispersion on UWB waveforms via optical pulse shaping techniques," *IEEE Trans. Microwave Theory and Tech.* **54**, 1681-1686 (2006).
18. T. Fortier, A. Bartels, and S. A. Diddams, "Octave-spanning Ti:sapphire laser with a repetition rate > 1 GHz for optical frequency measurements and comparisons," *Opt. Lett.* **31**, 1011-1013 (2006).
19. D.A. Braje, M. S. Kirchner, S. Osterman, T. M. Fortier, and S. A. Diddams, "Astronomical spectrograph calibration with broad-spectrum frequency combs," *Eur. J. Phys D* **48**, 57-66 (2008).
20. Mention of specific products and trade names is for technical communication only and does not constitute an endorsement by NIST.
21. T. Sizer, "Increase in laser repetition rate by spectral selection," *IEEE J. Quantum Electron.* **25**, 97-103 (1989).
22. E. N. Ivanov, S. A. Diddams, and L. Hollberg, "Experimental study of noise properties of a Ti:sapphire femtosecond laser," *IEEE Trans. Ultrasonics, Ferroelectrics and Freq. Control* **50**, 355-360 (2003).
23. T. M. Niebauer, R. Schilling, K. Danzmann, A. Rüdiger, and W. Winkler, "Nonstationary shot noise and its effect on the sensitivity of interferometers," *Phys. Rev. A* **43**, 5022-5029 (1991).
24. P. J. Winzer, "Shot-noise formula for time-varying photon rates: a general derivation," *J. Opt. Soc. Am. B* **14**, 2424-2429 (1997).
25. W. R. Bennett, *Electrical Noise*, Mc-Graw Hill (New York, 1960), and references therein.
26. F. Ma, S. Wang, and J. C. Campbell, "Shot noise suppression in avalanche photodiodes," *Phys. Rev. Lett.* **95**, 176604 (2005).

1. Introduction

A self-referenced femtosecond laser frequency combs that is stabilized to a high finesse optical cavity can be a source of microwave signals possessing very low phase noise [1, 2]. In such an approach, the femtosecond laser frequency comb functions as an optical-to-microwave frequency divider that transfers the low phase noise properties of a narrow linewidth continuous wave (CW) laser to the repetition rate, f_{rep} , of the femtosecond laser. Photodetection of this optical pulse train results in a corresponding train of current pulses, which in turn provides a comb of microwave frequencies at f_{rep} and its harmonics. Selection of any specific harmonic (e.g. at 10 GHz) is readily accomplished with a microwave filter. One advantage of this phase-coherent frequency division is the anticipated improvement to the microwave phase noise by $-20\log(N)$, where $N \sim 50,000$ is the division factor in going from the optical (500 THz) to the microwave (10 GHz) domain. In the division of an optical frequency to a 10 GHz carrier, we demonstrated residual single side-band phase noise of $L(f) = -110$ dBc/Hz at $f = 1$ Hz, reaching the shot-noise limited noise floor of $L(f) = -158$ dBc/Hz for $f > 100$ kHz [2]. Close to the microwave carrier this performance is approximately 40dB better than is achieved with traditional high quality microwave sources. The optical frequency divider concept has significant advantages over electronic methods in terms of low phase noise and low timing jitter, but the method has not yet achieved its full potential, in part due to the limitations of photodetectors addressed in this paper. We note that low-noise X-band (and higher frequency) microwave signals are of practical interest because they are well matched to available electronics with applications in radar[3], telecommunications, advanced clocks[4], high-speed sampling, and microwave photonics systems[5]. In the time domain, the low phase-noise achievable with the system demonstrated here gives timing resolution and timing jitter at the sub-femtosecond level[2]. In addition to low phase-noise and precise timing the microwave comb produced upon

photodetection could prove useful in microwave synthesis and in time domain generation of well controlled picosecond electrical signals.

However, challenges associated with the detection of high peak power, sub-picosecond optical pulses pose limitations to this approach. In earlier works we have identified beam pointing and amplitude fluctuations on the light as sources of excess phase noise[6, 7]. Here we focus on the degradation of the electrical signal-to-noise ratio due to saturation and pulse distortion effects in the photodiodes. Generally speaking, saturation behavior in P-I-N photodiodes degrades the temporal response of the resulting electrical pulses, such that they no longer efficiently generate a uniform microwave comb of frequencies. For example, we observe that increasing optical power does not result in an increase in the microwave power of the 10 GHz harmonic of the detected pulse train. This problem is exacerbated by the fact that the average photocurrent continues to increase with optical power, resulting in an increase in the photodetected shot-noise power which sets the noise floor for the microwave signals. Thus, one is in the unfortunate position of having the signal-to-noise ratio *decrease* with increasing light power on the photodetector.

High speed photodiodes capable of handling relatively large photocurrents are important for many applications and their saturation behavior has been studied previously [8, 9, 10, 11, 12]. Mechanisms responsible for saturation include space-charge fields and limited output voltage. In our case, the repetition rate, pulse duration and pulse energy of the laser are not well matched to the photodiode temporal response and the desired microwave frequency. From the time domain perspective, the use of a low rate (1 GHz) pulse train to drive a high rate (10 GHz) microwave signal unnecessarily increases the peak optical power and hastens the onset of saturation. To overcome this problem, we optically filter the frequency comb using a Fabry-Perot cavity with free-spectral-range (FSR) that is matched to a harmonic, N , of the 1 GHz source laser. Results shown here are for filter cavities having FSRs of 2, 5 and 10 GHz. In the frequency domain, the light transmitted through the filter cavity has a factor of N fewer optical modes. This corresponds to a time-domain multiplication of the pulse repetition rate by the same factor and a corresponding reduction in the average power and pulse energy by factors of N and N^2 , respectively. While the filtering process is inefficient, in that most of the incoming laser power is reflected back towards the source and never reaches the photodiode, we find that this approach leads to reduced saturation effects in the detected higher repetition rate pulse train, and permits significantly larger (+10 to +15 dB) microwave signals to be generated for the same average photocurrent. As the average photocurrent determines the fundamental detector shot noise power, this approach provides a net win in terms of signal-to-noise ratio.

The work reported here is similar in some respects to previous experiments in which pulse trains were used to reduce saturation effects in optical-to-electrical conversion in the THz regime[13, 14]. In the previous work optical pulse shaping was used to convert individual ultrashort pulses into bursts of evenly spaced pulses with reduced peak power, which were used to gate photoconductive antennas for generation of pulsed THz radiation. The power spectral density at selected THz frequencies was increased by up to 7.5 times compared to the saturated value under single pulse excitation. Compared to the current experiments, one difference is that in [13, 14] the pulse shaper was operated at low spectral resolution, leading to low duty cycle, isolated pulse bursts and continuous THz spectra. In contrast, the cavity filtering reported here operates at high spectral resolution on individual spectral lines, leading to 100% duty cycle waveforms and discrete RF spectra.

We also note that an alternative approach to cavity filtering could employ a pulse shaper for modulating the optical power spectrum on a coarse frequency scale coupled with a dispersive frequency-to-time converter. This approach has been used successfully for ultrawideband RF arbitrary waveform generation [15, 16, 17]. It should be possible to program such an RF wave-

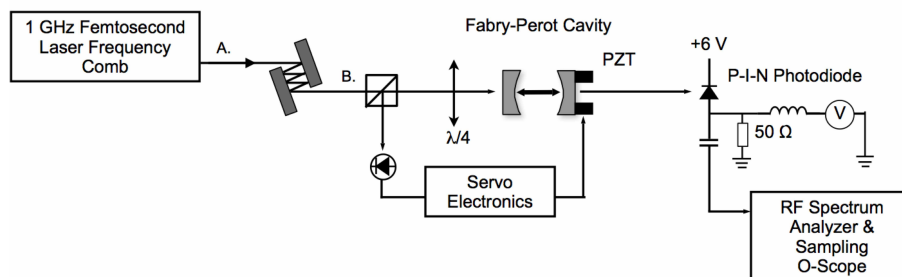


Fig. 1. Experimental setup. A 1 GHz, octave-spanning femtosecond Ti:sapphire laser is spectrally filtered with a Fabry-Perot cavity. Light reflected off the cavity is used to lock the Fabry-Perot on resonance with the laser frequency comb. The filter cavity output is detected with a P-I-N photodiode, and a bias-T is used to separate the direct and alternating currents.

form generator such that each individual ultrashort pulse is shaped and stretched into a 1 ns duration burst that is intensity modulated sinusoidally at the desired 10 GHz rate. The combined response from a 1 GHz input pulse train would correspond to a 100% duty cycle optical waveform with 10 GHz intensity modulation, while retaining a significantly higher fraction of the input optical power compared to the 10 GHz cavity filter. However, the pulse shaper might introduce some additional phase noise and timing jitter.

2. Cavity filtering

A schematic of the experimental setup is shown in Fig. 2. We employ a broad bandwidth femtosecond Ti:sapphire laser that operates at a repetition rate of 1 GHz [18]. The optical spectrum from the laser spans an octave, as shown in Fig. 2(a), thus permitting detection of the carrier-envelope-offset frequency f_{ceo} as required for stabilization of the underlying optical frequency comb. The associated frequency comb and laser repetition rate can be stabilized to light from a narrow-linewidth CW laser as required for low noise microwave generation [1, 2, 18]. A portion of the laser spectrum covering about 800-1000 nm is split from the total laser output using a dichroic beamsplitter. The spectral envelope is first shaped by multiple bounces off two flat dielectric mirrors centered at 910 nm ($R=99\%$). Then, the beam is spatially mode-matched to a Fabry-Perot cavity constructed from a pair of the same 910 nm mirrors, both having radii of curvature of 50 cm.

The length of the Fabry-Perot cavity can be easily changed over many centimeters such that the FSR is varied from 2 to 20 GHz. Once a specific harmonic is chosen, the length of the Fabry-Perot is locked to the input frequency comb using a PZT-mounted mirror and the standard dither and demodulation technique. Typical input and output spectral envelopes for the filter cavity set at 10 GHz are shown in Fig. 2(b). The coupling ratio P_{out}/P_{in} demonstrates that ~ 125 nm of spectral bandwidth is filtered with efficiency near 50%, which is in reasonably good agreement with the estimate given below. The output spectrum does not change significantly with Fabry-Perot FSR, although optimal spatial mode-matching requires adjustment of the input beam parameters. The light transmitted through the cavity is then focused onto a high-speed InGaAs P-I-N photodiode (Discovery 40s [20]), having responsivity of ~ 0.3 A/W in this spectral region. The duration of the transmitted optical pulses was measured with a nonlinear autocorrelator and found to be less than 1 ps, which is significantly less than the photodiode response time of ~ 40 ps. The photodiode is reverse biased with 6 V from a battery and the output current is coupled through a high bandwidth bias-T as indicated in Fig. 2. This provides

a convenient means for measuring the average photocurrent in the voltage drop across the internal 50 Ohm resistor, while the high frequency components of the photocurrent are capacitively coupled and available for analysis with a microwave spectrum analyzer and a 50 GHz bandwidth sampling oscilloscope. While the results presented here are specific to the InGaAs P-I-N photodiode, we have carried out similar experiments with GaAs P-I-N and InGaAs Schottky photodiodes and found the general trends to be similar.

The parameters of the filter cavity were selected based primarily on two design criteria: (1) the cavity bandwidth should be large in order to transmit as much of the input spectrum (and power) as possible; and (2) the intensities of the output pulses after repetition rate multiplication should be sufficiently uniform in order to maximize the microwave power at the desired harmonic—10 GHz in this case. With respect to the first criterion, the cavity bandwidth is limited by dispersion, which causes the frequencies of the cavity transmission resonances to deviate from those of the perfect frequency comb we wish to transmit. Assuming that the cavity is exactly resonant with the comb around some reference frequency ν_0 , the deviation $\delta\nu$ of the cavity resonance from the corresponding comb frequency at frequency ν is given by

$$|\delta\nu| = \frac{\Psi(\nu)c}{2\pi L}, \quad (1)$$

where L is the spacing of the two mirror cavity and $\Psi(\nu)$ is the spectral phase associated with the cavity dispersion (i.e., quadratic and higher-order spectral phase). A simple criterion for estimating the cavity bandwidth is setting the maximum permissible value of $\delta\nu$ equal to the half-width (at half-maximum) of the transmission resonance. This gives

$$|\delta\nu| = \frac{c}{2LF}, \quad (2)$$

where $F = \pi/(1-R)$ is the finesse of a lossless cavity with power reflectivity R , assumed equal for each of the two cavity mirrors. Putting these results together shows that the filter passband is given by the spectral region for which

$$|\Psi(\nu)| \leq 1 - R. \quad (3)$$

Accordingly, we optimize the cavity bandwidth by minimizing its dispersion and by using relatively low mirror reflectivities (constrained however by the second criterion). For an air-filled cavity, the dispersion is dominated by the mirrors. We have performed simulations investigating transmission bandwidth vs. mirror reflectivity for a quarter-wave dielectric stack mirror design, which appears to be a favorable choice. $R=99\%$ mirrors gave the best results for our cavity design, and should provide an estimated transmission bandwidth of ~ 150 nm in the 900 nm region. Higher reflectivity sacrifices bandwidth due to the narrowing of the cavity linewidth, while lower reflectivity (achieved by fewer coating layers) simply results in a narrowing of the cavity reflectivity bandwidth. Detailed experimental characterization of the optical comb filtering performance using this 99% mirror cavity design is reported in [19].

With respect to the second criterion, one can show that the relative power of the individual pulses in the repetition-rate-multiplied output train from the filter cavity are given by

$$I_n = (1-R)^2 \left| \sum_{m=0}^{\infty} R^{n+mk} \right|^2 = \frac{R^{2n}(1-R)^2}{(1-R^k)^2} \quad (4)$$

where k is the repetition rate multiplication factor, and I_n is the relative power of the $(n+1)^{th}$ pulse within one period of the original (input) pulse train, where n takes on values $0, 1 \dots k-1$.

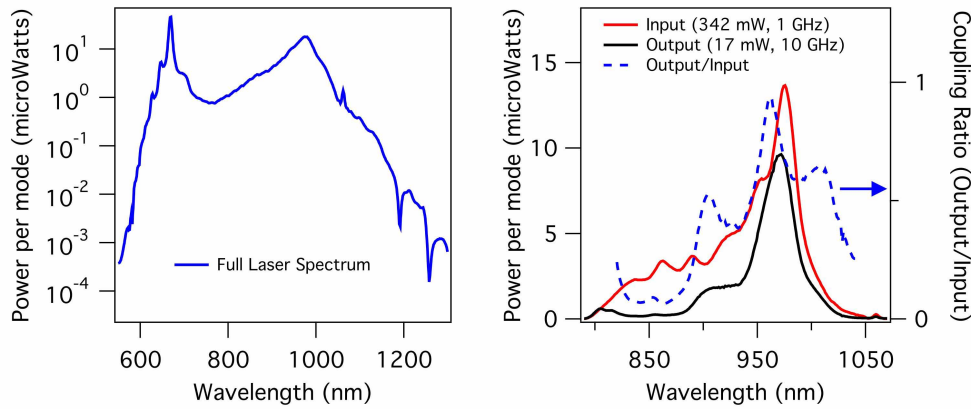


Fig. 2. (a) Full spectrum of the 1 GHz octave-spanning Ti:sapphire, measured at point A of Fig. 1. (b) Optical spectrum at $f_{rep} = 1$ GHz input to the optical filter cavity (red), measured at point B of Fig. 1. Optical spectrum at $f_{rep} = 10$ GHz output from the filter cavity (black). Coupling ratio, defined as P_{out}/P_{in} (blue dashed).

Here I_n is normalized to the power of the input pulse, and a lossless, symmetric, precisely resonant two mirror cavity is assumed. The RF spectral amplitude $V_{kf_{rep}}$ at the multiplied repetition rate is proportional to

$$V_{kf_{rep}} \sim \frac{1}{k} \sum_{n=0}^{k-1} I_n = \frac{1}{k} \frac{1 - R^{2k}}{1 - R^2} I_0 \quad (5)$$

If we assume that the saturation of the photodiode is determined by the power of the strongest pulse in the train (I_0), then the quantity $V_{kf_{rep}}/I_0$ serves as a natural metric for the penalty in RF generation due to nonuniformity in the repetition rate multiplied output (compared to an ideal equal power pulse train). The corresponding penalty in terms of RF power spectrum is expressed as

$$-20 \log_{10} \left[\left(\frac{1}{k} \right) \left(\frac{1 - R^{2k}}{1 - R^2} \right) \right] \quad (6)$$

For repetition rate multiplication from 1 to 10 GHz ($k = 10$) and mirror reflectivity $R=99\%$, the power penalty is only 0.77 dB. This justifies the use of relatively low (99%) reflectivity mirrors, given the large cavity bandwidth (and proportionally large output power) these mirrors provide.

3. Photodiode saturation

The saturation behavior of the InGaAs photodiode is illustrated in the complimentary time and frequency domain data of Fig. 3. For these data, the unfiltered 1 GHz pulse train was focused onto the photodiode. The average optical power was changed in discrete steps with a set of neutral density filters, and the microwave pulse train was analyzed with the high-speed sampling scope and the microwave spectrum analyzer. The time domain response of the photodiode to the short optical pulses is shown in Fig. 3(a). For average optical powers above a few milliwatts (average photocurrents < 1 mA), the electrical pulse begins to broaden significantly from the low power width of ~ 40 ps up to nearly 140 ps. This pulse broadening as a function of optical power is summarized in Fig. 3(b). The corresponding frequency-domain response is shown in Fig. 3(c)-(d). A microwave spectrum taken with 69.4 mW (19 mA average current) is shown in

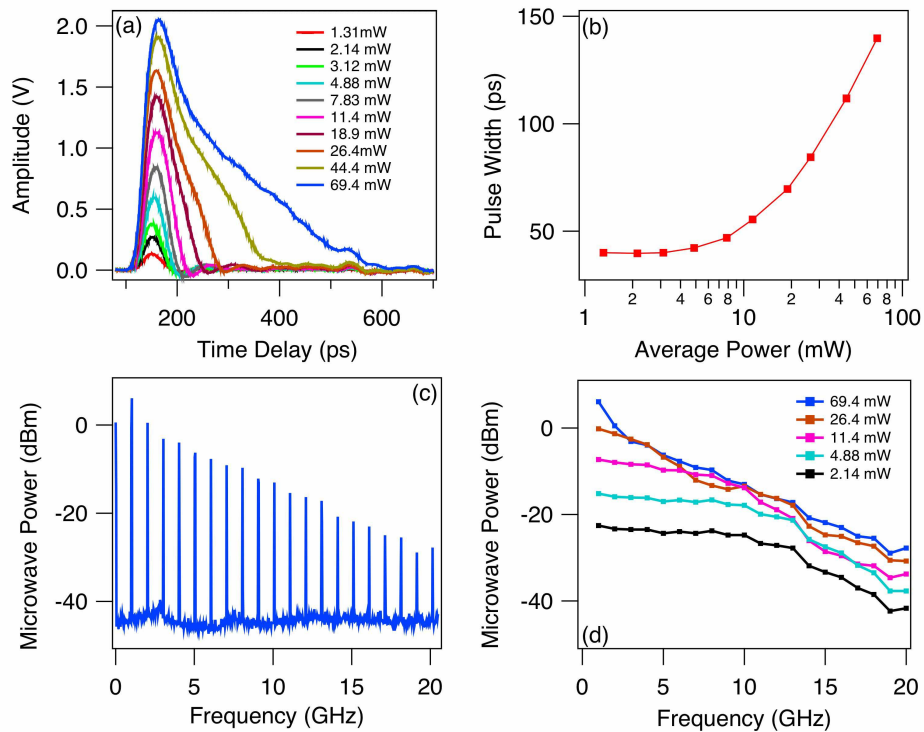


Fig. 3. (a) Electrical waveforms recorded with a 50 GHz sampling oscilloscope for different average optical powers of a 1 GHz pulse train. (b) Variation in measured pulse width as a function of average optical power. (c) Microwave spectrum of 1 GHz pulse train for average optical power of 69.4 mW. (d) Microwave power in harmonics of 1 GHz pulse train illustrating saturation of higher frequency harmonics.

Fig. 3(c), illustrating the strong roll-off for frequency components greater than a few gigahertz. Of particular interest, Fig. 3(d) shows that above ~ 10 mW of average power, there is no further increase in the 10 GHz microwave harmonic. Qualitatively speaking, this pulse distortion is similar to our earlier measurements [7] and is consistent with an excess of photocarriers that cannot be rapidly extracted, thereby leading to decreased bandwidth of the photodiode at high powers [10]. We note that we observe no evidence of saturation in the average photocurrent, which remains linearly proportional to the optical power over the full range of powers explored here.

4. Improved 10 GHz signal-to-noise with cavity filtering

The effects of the pulse distortion and microwave power saturation seen in Fig. 3 are reduced by the introduction of the Fabry-Perot filter cavity. Here we focus on the achievable power in the 10 GHz harmonic for filter cavity FSR's of 2, 5 and 10 GHz. For each filter cavity FSR, the microwave spectrum of the photocurrent is recorded for a range of optical powers. The results are summarized in Fig. 4, where the power in the 10 GHz harmonic is plotted as a function of average photocurrent for the three filter cavity FSRs, in addition to the un-filtered 1 GHz pulse train. In the linear regime, the 10 GHz power is proportional to the square of the photocurrent. This linear response is observed in all cases of filtering for average photocurrents < 1 mA.

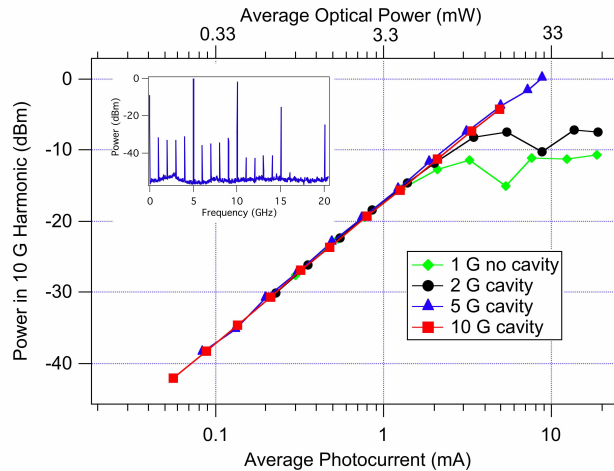


Fig. 4. Power in 10 GHz microwave harmonic as a function of average photocurrent (and optical power) for 1 GHz pulse train, and for the same pulse train after filtering with 2, 5 and 10 GHz Fabry-Perot cavities. The inset shows the full microwave spectrum for the case of the 5 GHz filter cavity with ~ 23 mW incident on the photodiode.

However, as already noted in Fig. 3, with illumination by the 1 GHz pulse train, saturation of the 10 GHz harmonic is observed above average photocurrents of ~ 2 mA. Filtering to 2 GHz improves the level of linearity by approximately a corresponding factor of 2. For filter cavities of 5 and 10 GHz, the linear regime of 10 GHz generation extends to still higher average photocurrents; however, for these cases there is not sufficient light power available after the filter cavity to clearly drive the photodiode into saturation. The highest 10 GHz power is achieved with the 5 GHz FSR filter cavity where nearly 30 mW of optical power is available to provide 8.7 mA of average photocurrent and power in the 10 GHz harmonic of +1 dBm, as measured by the microwave spectrum analyzer (corrected for system losses). We note that the AC photocurrent is divided between the 50 Ohm termination of the photodiode and the 50 Ohm input of the spectrum analyzer. With a single 50 Ohm termination, the voltage at 10 GHz might be doubled, resulting in a potential 6 dB increase in the usable 10 GHz microwave power. To further increase the available 10 GHz power it would be possible to use the reflected power off the front of the filter cavity[21]. This light could be filtered in a second cavity that is tuned to an adjacent set of 5 or 10 GHz optical modes. The filtered light would illuminate a second photodiode and the resulting photocurrent could be summed with that of the first detector. The process could be repeated with additional power gain per filter stage.

For the purpose of low noise microwave generation, the > 10 dB increase in 10 GHz signal realized by filtering the output of the 1 GHz frequency comb is significant. While signal size is important, often the more relevant parameter is the achievable signal-to-noise ratio of the 10 GHz signal. Close to the carrier, the noise of a frequency-stabilized mode-locked laser is typically dominated by unsuppressed frequency fluctuations arising from pump laser noise and acoustic noise [1, 2, 6]. However, beyond a few hundred kilohertz, the technical noise falls below that of fundamental noise processes, such as shot noise and thermal (Johnson) noise [2]. If the photodetected current is above a few milliamperes in a 50 Ohm systems, then the shot noise is dominant. The required dynamic range poses a challenge in measuring the far-from-carrier shot noise floor. Similar to an earlier measurement [22], we suppress the 10 GHz carrier using

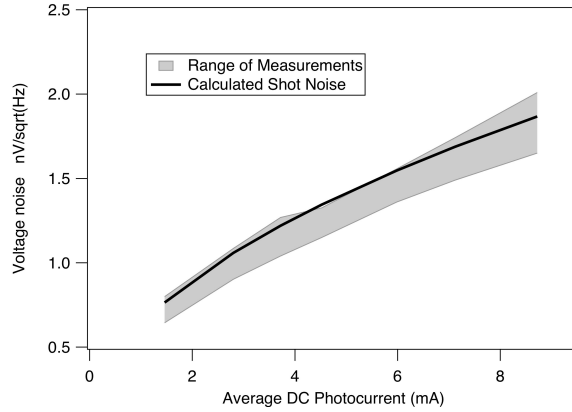


Fig. 5. The grey shaded region illustrates the maximum scatter of three separate measurements of the noise floor > 400 MHz from the 10 GHz carrier. The black line is the calculated shot-noise floor, assuming it depends on the average photocurrent.

a tunable microwave bandpass filter (~ 100 MHz bandwidth) centered at 9.5 GHz. The noise floor in the vicinity of 9.5 GHz is then amplified with a low noise microwave amplifier and the noise density is measured using the noise marker function of a microwave spectrum analyzer. The accuracy of the microwave spectrum analyzer was verified with a calibrated thermal noise source. Additionally, the voltage gain of the microwave amplifier and the loss of the tunable filter and coaxial cables were measured and accounted for. The grey shaded area of Fig. 5 shows the total range (scatter) of three different measurements. The agreement among the measurements at the level of 10-20% (< 1 dB) is reasonable given the nanovolt magnitude of the voltage noise and the uncertainties in calibration of the loss/gain in the components employed

These measured values are compared with the calculated photodetector shot noise floor. For simplicity, we assume that the shot noise voltage in a 1 Hz bandwidth is determined by the average photocurrent and the terminating resistor: $V_{sn} = R\sqrt{2ei_{avg}}$, where $R = 50$ Ohm, e is the electron charge, and i_{avg} is the average photocurrent. As pointed out below, because we are dealing with a time varying signal, there may be limitations to this assumption. Nonetheless, for the maximum achieved photocurrent of $i_{avg} = 8.7$ mA obtained with the 5 GHz FSR filter cavity, we calculate $V_{sn} = 2.6\text{nV}/\sqrt{\text{Hz}}$. As noted above, the AC current generated at the photodiode is divided between the internal 50 Ohm load and that of the microwave spectrum analyzer (or amplifier in this case). Thus, the measured shot noise floor at high frequencies corresponds to half the average current. When this factor of $\sqrt{2}$ is accounted for in the calculated shot noise, we obtain $V_{sn} = 1.8\text{nV}/\sqrt{\text{Hz}}$. The full set of calculated values is given by the black solid line in Fig. 5, which is found to be in good agreement with the measured noise. The measurement also roughly follows the same $\sqrt{i_{avg}}$ dependence of the calculation. This indicates that the measured noise is not simply excess amplitude noise, which would exhibit a linear relationship between average current and voltage noise. The measured shot noise voltage at 8.7 mA corresponds to a shot noise power of $P_{sn} = V_{sn}^2/R = -161\text{dBm/Hz}$. Considering the power in only one quadrature reduces this noise power to -164dBm/Hz . When combined with the 10 GHz signal of $+1\text{dBm}$, this implies that the cavity filtering approach demonstrated here could provide stable microwave signals with a fundamental phase noise floor power -165dB below the carrier, or equivalently $L_f = S_\phi - 3\text{dB} = -168\text{dBc/Hz}$.

5. Discussion and conclusion

In this paper, we have demonstrated that appropriate optical filtering of a femtosecond laser frequency comb can lead to improved temporal response in photodetection of the associated optical pulse train. This subsequently leads to an enhancement of the signal-to-noise ratio of desired microwave harmonics near 10 GHz. This approach should be beneficial in the photonic generation of low phase noise microwave signals with stabilized femtosecond frequency combs. It is of further interest to consider the limitations of this approach to the generation of 10 GHz microwave signals with low phase noise floor. If the photodiode remains in the linear regime, one would expect the 10 GHz signal power to continue to increase as the square of the photocurrent, while the power of the shot-noise floor increases linearly with photocurrent. This implies that the shot-noise limited signal-to-noise ratio also increases linearly with photocurrent. Further gains beyond those demonstrated here would require still greater laser power as well as photodiodes that fulfill the requirement of high-speed (10 GHz) linearity at currents above 10 mA. A relevant consideration in this discussion is the fact that the simple shot noise expression used here may have limitations when applied to time-varying signals—such as those obtained from the detection of an optical pulse train [23, 24]. Additionally, sub shot-noise behavior of vacuum diodes[25] and photodiodes[26] has been observed, and attributed in some cases, to space-charge effects and mechanisms that result in correlation of the photoelectrons. While the noise measurements presented here are consistent with the time-independent shot noise model, the precision is not sufficient to rule out more complicated—and interesting—noise phenomena.

Acknowledgments

We thank Nate Newbury and Shijun Xiao for their thoughtful comments on this manuscript. Financial support for this work was provided by DARPA and NIST. This work is a contribution of an agency of the US Gov't and is not subject to copyright in the US.